

Zwitterionic [4]Helicene: an Hydrosoluble and Reversible pH-Triggered ECD/CPL Chiroptical Switch in the UV and Red Spectral Regions

Simon Pascal, Céline Besnard, Francesco Zinna, Lorenzo Di Bari,
Boris Le Guennic, Denis Jacquemin, and Jérôme Lacour*

Electronic Supporting Information

1. GENERAL REMARKS AND METHODS.....	S2
2. X-RAY CRYSTALLOGRAPHY	S4
3. SOLUBILITY STUDY IN ACIDIC AND BASIC AQUEOUS SOLUTIONS.....	S6
4. CHARACTERIZATION OF <i>M</i> AND <i>P</i> ENANTIOMERS	S7
5. ADDITIONAL OPTICAL AND CHIROPTICAL DATA	S8
6. ADDITIONAL THEORETICAL DATA	S11
7. REFERENCES	S13

1. General remarks and methods

Synthesis. Compounds **5** and **6** were prepared following reported procedures.¹ Resolution of **1** was carried using (+)-(*R*)-methyl-*p*-tolyl sulfoxide and following a reported protocol.²

Analytical methods and apparatus. UV-vis-NIR absorption spectra were recorded on a JASCO V-650 spectrophotometer at 20°C. Optical rotation were measured on a Perkin Elmer 241 polarimeter at 20°C using a HG lamp (365 nm). Electronic circular dichroism spectra were recorded on a JASCO J-815 spectrophotometer at 20°C.

Crystallography. All data were collected on an Agilent supernova dual source diffractometer equipped with an Atlas detector, using Cu K α radiation. Data reduction was carried out in the crysalis Pro Software.³ Structure solution was made using direct methods (sir2004⁵). Refinements were carried out in Shexl⁴ within the Olex2⁷ software.

Luminescence. Steady-state fluorescence spectra were measured using a Varian Cary 50 Eclipse spectrofluorimeter. All fluorescence spectra were corrected for the wavelength-dependent sensitivity of the detection. Fluorescence quantum yields Φ were measured in diluted solution with an optical density lower than 0.1 using the following equation:

$$\frac{\Phi_x}{\Phi_r} = \left(\frac{A_r(\lambda)}{A_x(\lambda)} \right) \left(\frac{n_x^2}{n_r^2} \right) \left(\frac{D_x}{D_r} \right)$$

where A is the absorbance at the excitation wavelength (λ), n the refractive index and D the integrated intensity. "r" and "x" stand for reference and sample. The fluorescence quantum yields were measured relative to cresyl violet in methanol ($\Phi = 0.54$). Excitation of reference and sample compounds was performed at the same wavelength. Short luminescence decay was monitored using a Horiba-Jobin-Yvon Fluorolog-3 iHR320 fluorimeter equipped with the TC-SPC Horiba apparatus and using Ludox in distilled water to determine the instrumental response function used for deconvolution. Excitation was performed using a 570 nm NanoLED (peak wavelength: 573 nm; pulse duration: 1.5 ns), and the deconvolution was performed using the DAS6 fluorescence-decay analysis software.

pKa determination. The absorption spectra of the [4]-helicene ($c = 1.036 \cdot 10^{-5}$ M) was investigated in aqueous solution with pH ranging from 0.40 to 7.03. The pKa was determined by monitoring pH-dependence of the absorbance at 630 nm and using the following equation:

$$pKa = pH_i - \log \left(\frac{A_{HA} - A_i}{A_i - A_{A^-}} \right)$$

with HA and A⁻ being respectively the carboxylic and carboxylate forms of the dye.

Circularly polarized luminescence. All the circularly polarized luminescence (CPL) measurements were performed using our home-built CPL spectrofluoropolarimeter (see below for a description). The samples were excited using a 90° geometry with a green InGaN (3 mm, 2 V) LED source (Lucky light Electronics Co., LTD, $\lambda_{\max} = 517$ nm, HWHM = 15 nm). We used the following parameters: emission slit width ≈ 10 nm, integration time = 4 sec, scan speed = 60 nm/min, accumulations = 8.

The concentration of all the samples was $2/3 \cdot 10^{-5}$ M. The spectra were baseline corrected by subtracting the spectrum of the racemic mixture.

The instrument was built using the chassis, photoelastic modulator (PEM, Jasco, modulated at 50 KHz), lock-in amplifier and photomultiplier tube (end-on PMT, Hamamatsu R376) of a decommissioned Jasco J-500 C spectropolarimeter. The PEM, followed by a linear polarizer, is placed in front of the sample holder. The light then passes through a Jasco CT-10 monochromator (1200 grooves/mm blazed at 500 nm) driven by a step motor controlled by an electronic prototyping platform. The same platform digitalizes the analog output signals (both direct and alternate current signals). The spectra are plotted in real time in an Excel spreadsheet. A full description of the instrument will be given in a forthcoming publication.

Calculation methods. DFT and TD-DFT calculations on molecules were carried out with the Gaussian 09 program package,⁸ applying both a tightened self-consistent field convergence criterion (10^{-9} - 10^{-10} au) and an improved optimization threshold (10^{-5} au on average forces). For each molecule, we have optimized the geometry of the ground electronic state and computed its vibrational spectra to ascertain the nature of the optimized structure. Next, the geometry and vibrational frequencies of the lowest excited-state were determined with TD-DFT. The same DFT integration grid, namely the so-called *ultrafine* pruned (99,590) grid, was used for all calculations. All DFT and TD-DFT structural calculations were performed with the M06-2X *meta*-GGA hybrid exchange–correlation functional⁹ that has been shown to be an adequate choice for investigating structures of both ground and excited-states of many classes of molecules.¹⁰ The CT parameters and MOs have been determined with the same functional, whereas B3LYP was used to determine the ECD spectra, a choice justified by previous benchmarks.¹¹ The structural parameters were determined with the 6-31G(d) atomic basis set whereas the transition energies have been obtained with the more extended 6-311+G(2d,p) atomic basis set. When necessary, bulk solvation effects (here acetonitrile) have been quantified using the Polarizable Continuum Model (PCM).¹² The structural and vibrational parameters of the excited-state were obtained in the linear-response (LR) PCM model,¹³ considering the so-called *equilibrium* limit. To determine the absorption and emission energies, we have applied the corrected LR (cLR) PCM approach¹⁴ in its *non-equilibrium* limit as this protocol is suited to investigate rapid transitions. The protocol used to obtain the 0-0 energies has been described previously.¹⁵ We have determined $\Delta\rho$ plots and associated charge-transfer (CT) parameters following the procedure defined by Le Bahers and coworkers,¹⁶ whereas the reported partial atomic charges (simply referred to as charge in the body of the text) correspond to the so-called Merz-Kollman model. The (gas phase) SOS-CIS(D) calculations have been performed with the Q-Chem code¹⁷ using the 6-311+G(2d,p) basis set, whereas CC2 calculations were obtained with the Turbomole program¹⁸ using the *aug-cc-pVDZ* atomic basis set.

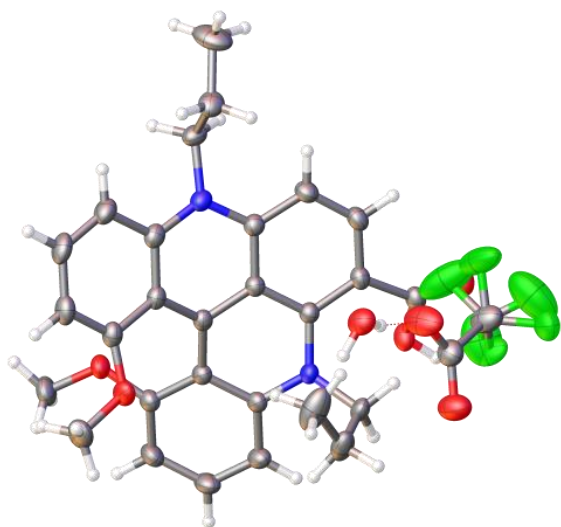
2. X-ray crystallography

Details for the refinement for the structure can be found below with a representation of the asymmetric units shown as displacement ellipsoids, drawn as 50 percent probability and a picture of the packing.

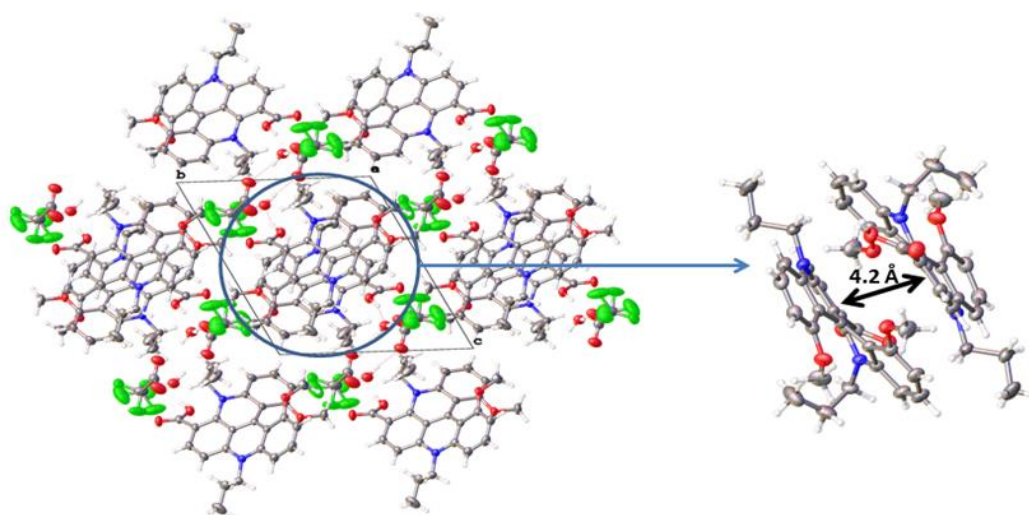
Table S 1. Crystal data and structure refinement for **6-H**.

CCDC number	1472769
Empirical formula	$C_{30}H_{31}F_3N_2O_7$
Formula weight	588.57
Temperature/K	180(2)
Crystal system	triclinic
Space group	P-1
a/Å	10.9257(5)
b/Å	12.2016(4)
c/Å	12.7292(4)
$\alpha/^\circ$	111.624(3)
$\beta/^\circ$	97.490(3)
$\gamma/^\circ$	110.940(4)
Volume/Å ³	1404.61(10)
Z	2
$\rho_{\text{calc}}/\text{cm}^3$	1.392
μ/mm^{-1}	0.952
F(000)	616.0
Crystal size/mm ³	0.5829 × 0.24 × 0.1579
Radiation	CuK α ($\lambda = 1.5418$)
2 θ range for data collection/ $^\circ$	7.836 to 146.79
Index ranges	-11 ≤ h ≤ 13, -15 ≤ k ≤ 15, -15 ≤ l ≤ 15
Reflections collected	21587
Independent reflections	5561 [$R_{\text{int}} = 0.0349$, $R_{\text{sigma}} = 0.0230$]
Data/restraints/parameters	5561/56/420
Goodness-of-fit on F^2	1.061
Final R indexes [$I \geq 2\sigma(I)$]	$R_1 = 0.0465$, $wR_2 = 0.1259$
Final R indexes [all data]	$R_1 = 0.0514$, $wR_2 = 0.1309$
Largest diff. peak/hole / e Å ⁻³	0.28/-0.36

View of the asymmetric unit. The anisotropic displacement ellipsoids are drawn at 50 percent probability.



The trifluoroacetate anion is disordered and was refined using six fluorine atoms. Restraints were applied on 1-2 and 1-3 distances and on anisotropic displacement parameters. Hydrogen atoms bound to O were refined using distances restraints.



Packing of the Crystals. View along the a direction (left) where the molecules form stack. The distance between neighbouring molecules inside the stack is about 4.2 Å (right)

3. Solubility study in acidic and basic aqueous solutions

Absorption spectra were measured for several dilutions of a same mother solution either in 1M aqueous HCl (aggregation observed beyond $9.98 \cdot 10^{-5}$ M) or NaOH (aggregation observed beyond $3.74 \cdot 10^{-4}$ M).

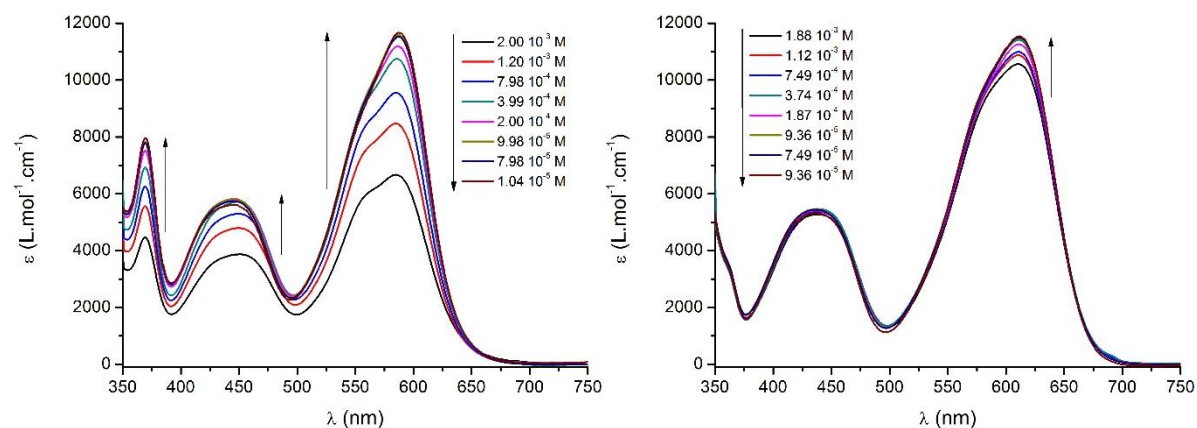


Figure S1. Concentration-dependent absorption spectra of compound **6/6-H** in 1M aqueous HCl (left) and NaOH (right) solutions.

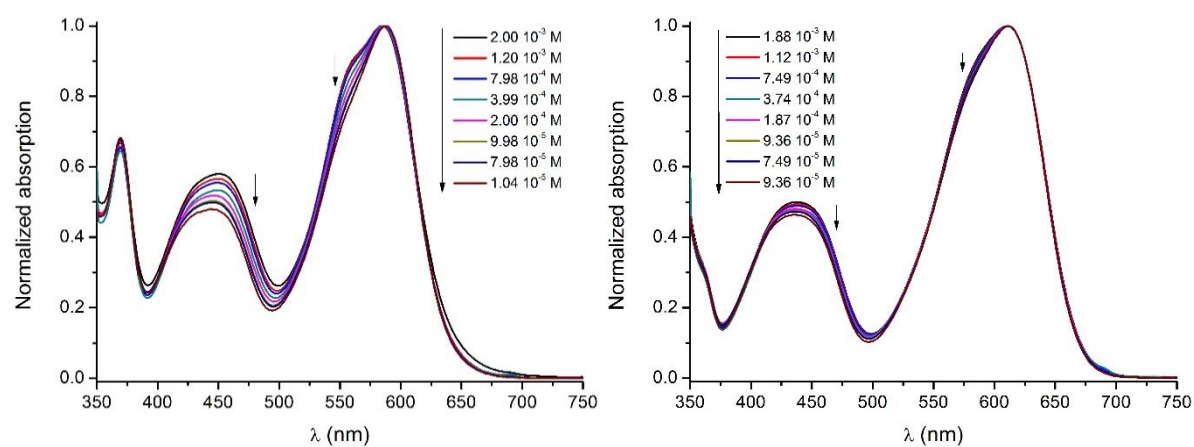
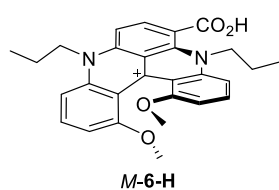


Figure S2. Concentration-dependent normalized absorption spectra of compound **6/6-H** in 1M aqueous HCl (left) and NaOH (right) solutions.

4. Characterization of *M* and *P* enantiomers

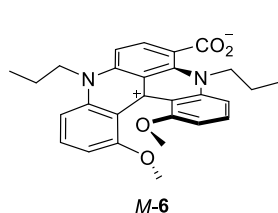
Cationic [4]helicenes are dyes that absorb light efficiently in most of the visible region, leading to high errors during OR measurements. Thus very dilute solutions and restricted wavelengths were required to measure the specific optical rotations with Hg lamp.^{16,2} During ECD and reversibility measurements, small aliquots of concentrated HBF₄ or pure Et₃N (*ca.* 5 μ L) were added to a 25 mL solution of the dye in CH₃CN (final concentration *ca.* 2.10⁻⁵ M) to ensure strongly acidic and basic conditions.

Optical data



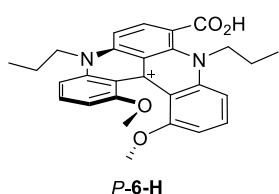
In CH₃CN+HBF₄: **CD** (1.18.10⁻⁵ M, 20°C) λ ($\Delta\epsilon$) 600 (-3.5), 463 (7.8), 407 (-2.8), 366 (4.6), 329 (-7.2), 301 (-39.5). **OR** $[\alpha]_{365} = -5300$ ($c = 6.44.10^{-6}$ g.mL⁻¹, 20°C).

In HCl 1M: **CD** (1.04.10⁻⁵ M, 20°C) λ ($\Delta\epsilon$) 602 (-3.1), 461 (6.8), 408 (-1.8), 367 (5.1), 302 (-38.8). **OR** $[\alpha]_{365} = -5600$ ($c = 5.68.10^{-6}$ g.mL⁻¹, 20°C).



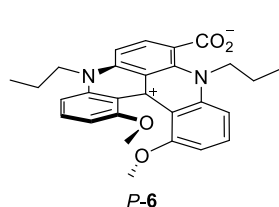
In CH₃CN+Et₃N: **CD** (1.18.10⁻⁵ M, 20°C) λ ($\Delta\epsilon$) 665 (-3.0), 457 (8.0), 400 (-2.3), 331 (-20.2), 309 (8.2), 282 (-52.8). **OR** $[\alpha]_{365} = -7000$ ($c = 6.44.10^{-6}$ g.mL⁻¹, 20°C).

In NaOH 1M: **CD** (1.04.10⁻⁵ M, 20°C) λ ($\Delta\epsilon$) 628 (-3.0), 457 (7.0), 406 (-1.7), 322 (-15.0), 284 (-42.0). **OR** $[\alpha]_{365} = -4900$ ($c = 5.68.10^{-6}$ g.mL⁻¹, 20°C).



In CH₃CN+HBF₄: **CD** (1.15.10⁻⁵ M, 20°C) λ ($\Delta\epsilon$) 603 (3.5), 466 (-8.7), 409 (2.2), 365 (-6.7), 328 (6.2), 300 (43.9). **OR** $[\alpha]_{365} = +3700$ ($c = 6.24.10^{-6}$ g.mL⁻¹, 20°C).

In HCl 1M: **CD** (1.17.10⁻⁵ M, 20°C) λ ($\Delta\epsilon$) 606 (3.7), 464 (-7.4), 406 (2.1), 367 (-6.7), 325 (8.5), 303 (45.7). **OR** $[\alpha]_{365} = +5500$ ($c = 6.36.10^{-6}$ g.mL⁻¹, 20°C).



In CH₃CN+Et₃N: **CD** (1.15.10⁻⁵ M, 20°C) λ ($\Delta\epsilon$) 649 (3.0), 453 (-7.7), 403 (2.3), 330 (20.1), 310 (-7.1), 282 (52.5). **OR** $[\alpha]_{365} = +5600$ ($c = 6.24.10^{-6}$ g.mL⁻¹, 20°C).

In NaOH 1M: **CD** (1.17.10⁻⁵ M, 20°C) λ ($\Delta\epsilon$) 616 (3.9), 458 (-8.8), 401 (1.4), 321 (15.0), 311 (7.6), 284 (46.3). **OR** $[\alpha]_{365} = +5300$ ($c = 6.36.10^{-6}$ g.mL⁻¹, 20°C).

5. Additional optical and chiroptical data

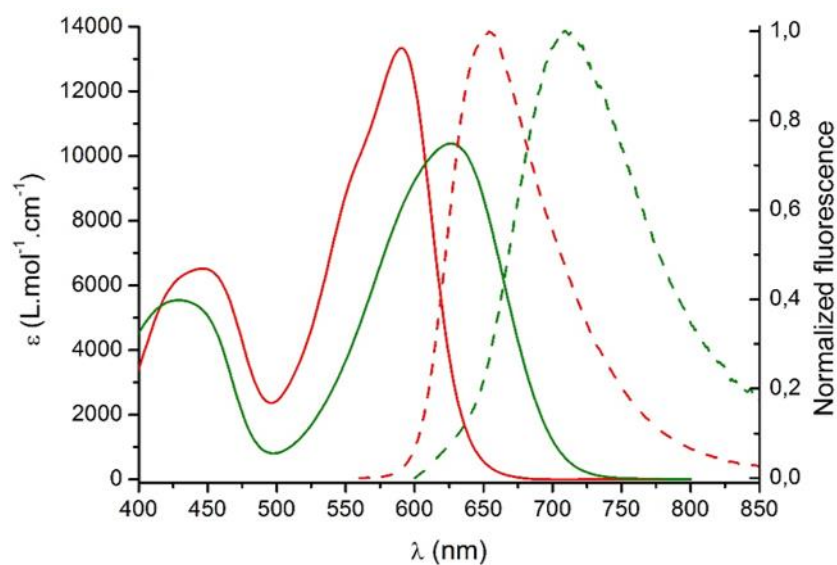


Figure S3. Absorption (plain) and normalized fluorescence (dash) spectra of compound **6/6-H** in acetonitrile in presence of HBF_4 (red) or Et_3N (green).

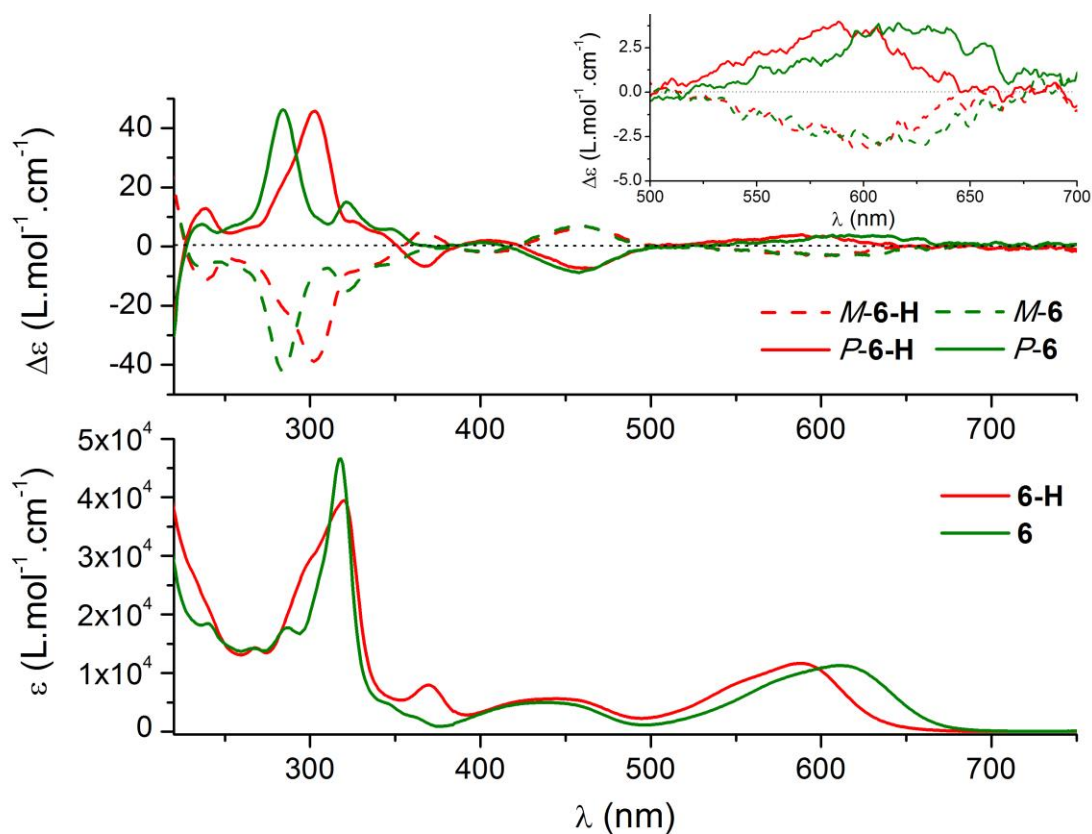


Figure S4. Circular dichroism (top) and absorption (bottom) spectra of compound **6/6-H** in aqueous solution (ca. 10^{-5} M; red: HCl 1 M; green: NaOH 1 M). The inset is a zoom of the green to red spectral region of the ECD spectra.

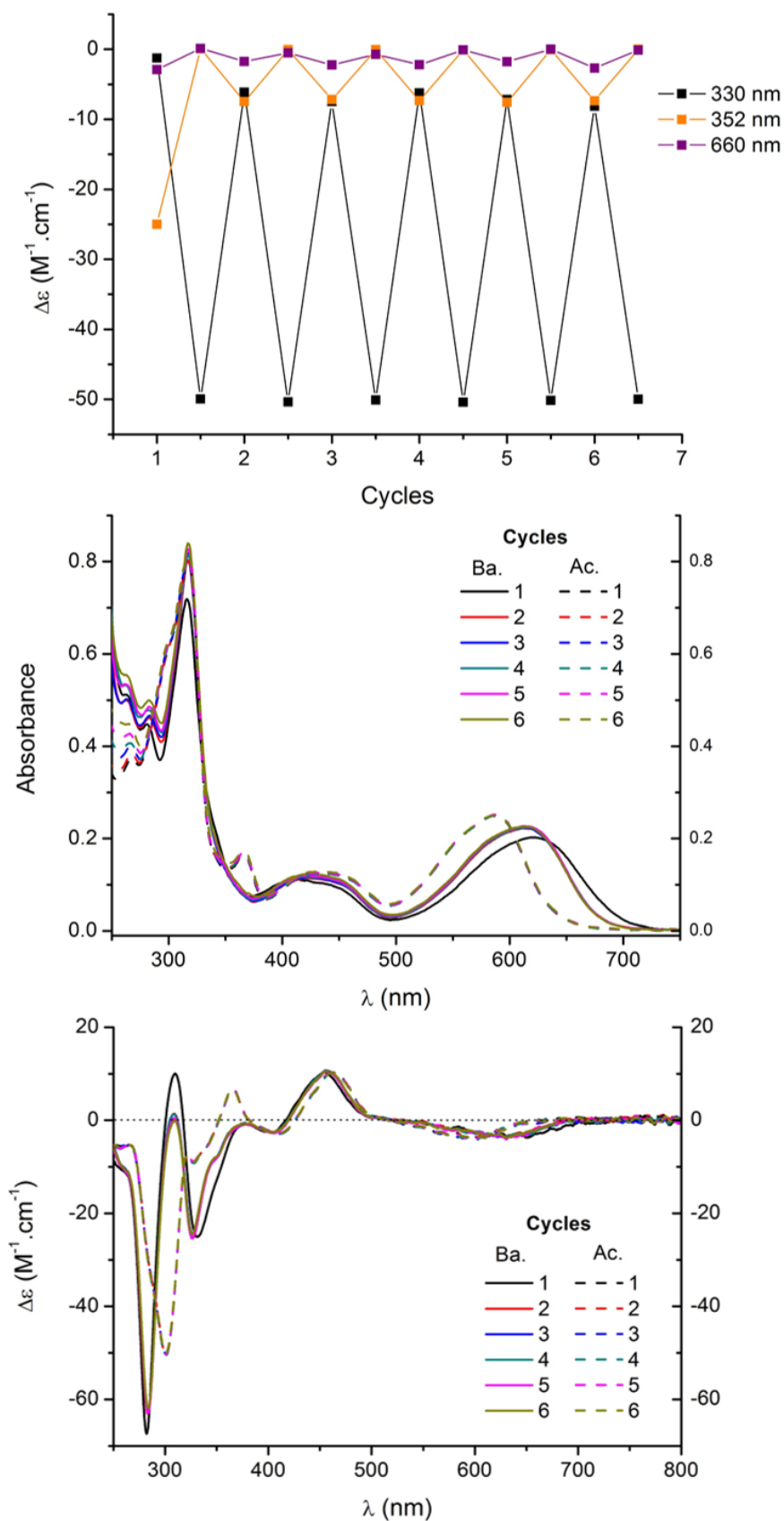


Figure S5. Reversibility tests of *M-6/6-H* pH-switching (top), monitored by UV-Vis absorption (middle) and ECD (bottom). The low ECD signal observed for the zwitterionic form after the first cycle is due to the presence of water after introduction of an aliquot of concentrated aqueous HBF_4 within the acetonitrile solution and resulting in a slight red-shift of the band.

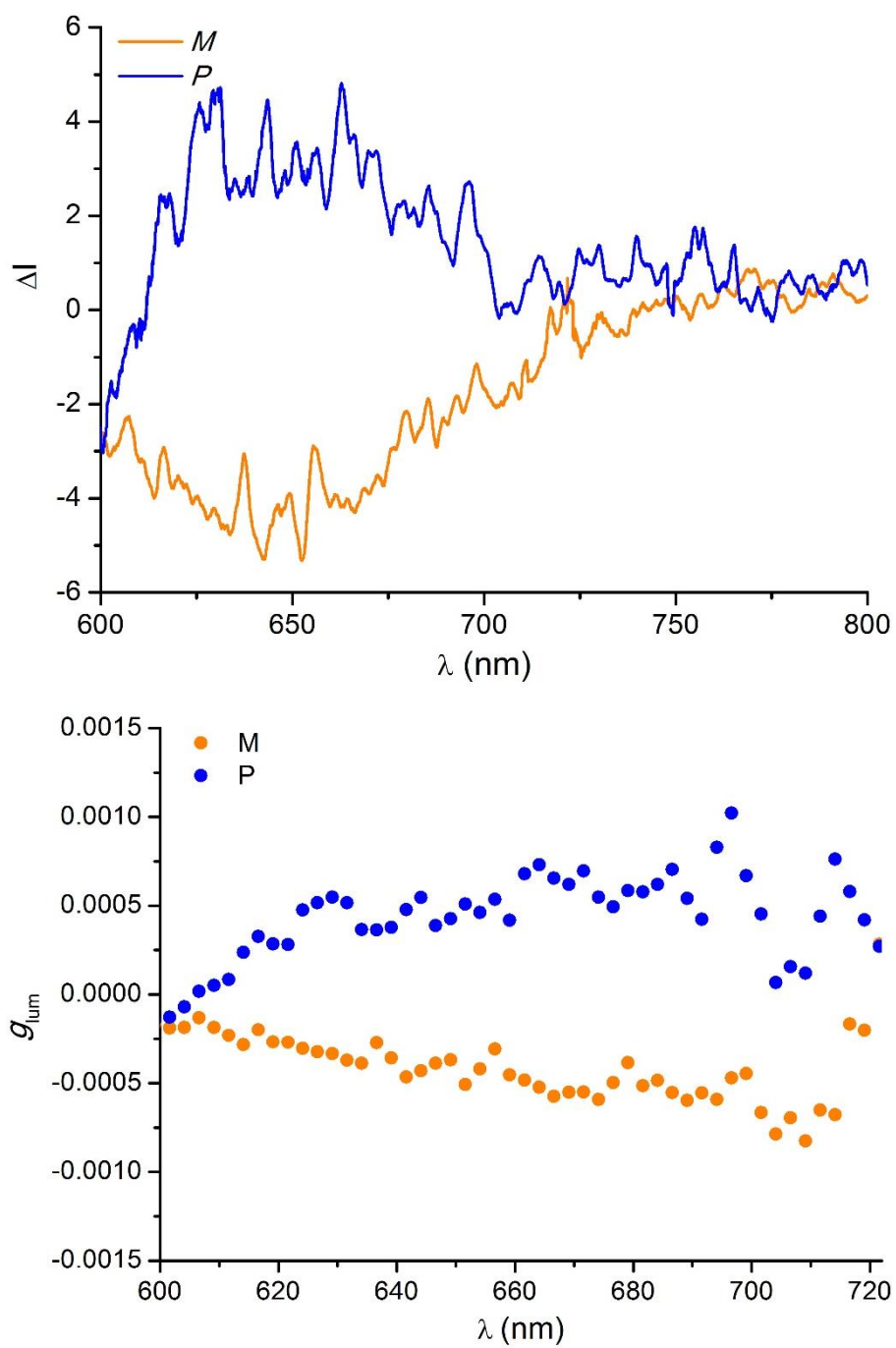


Figure S6. CPL spectra (top) and g_{lum} response (bottom) of the two enantiomers of **6** in aqueous solution (HCl 1 M).

6. Additional theoretical data

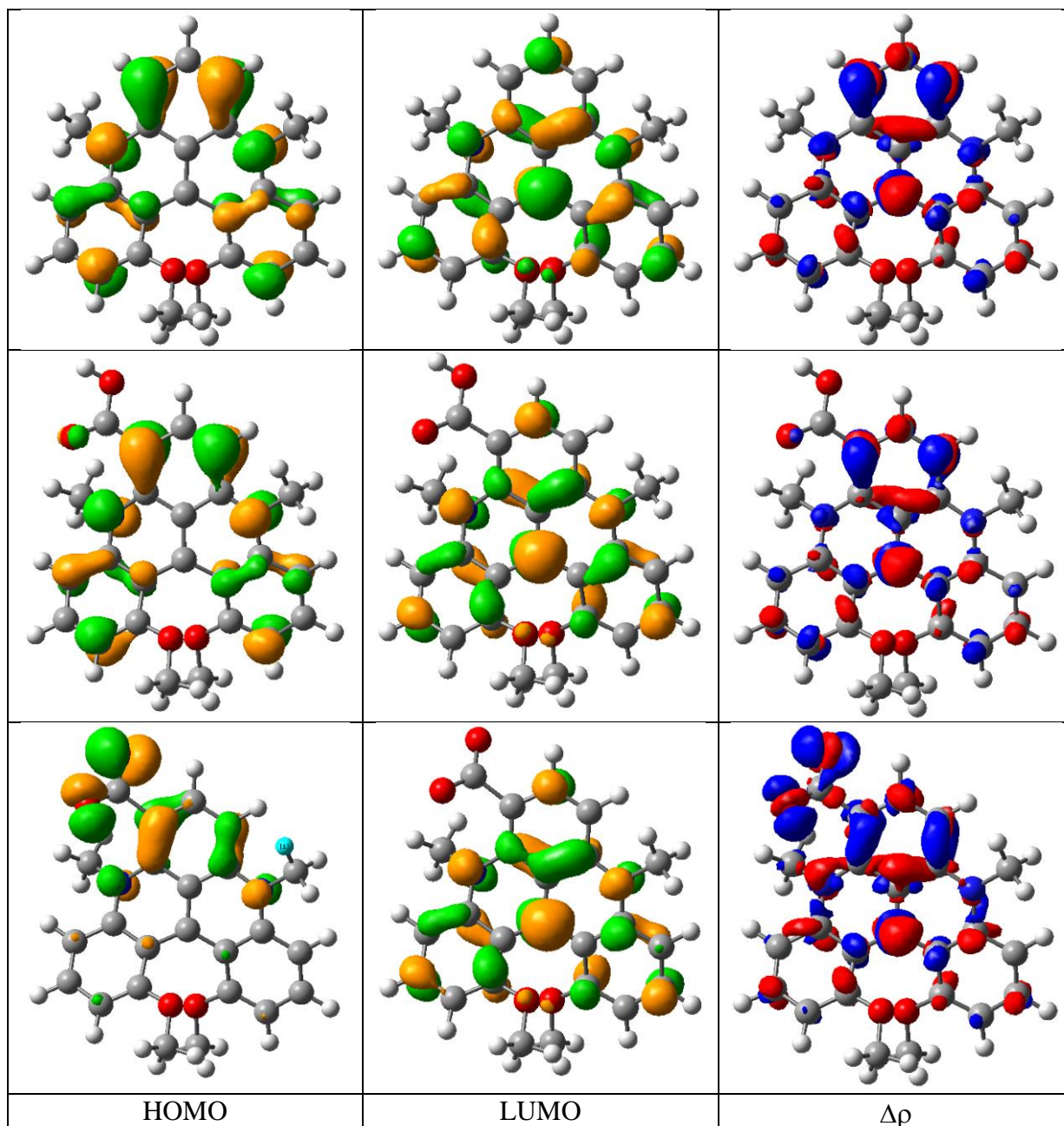


Figure S7. Representation of the frontier orbitals (contour threshold 0.040 au) and delta density plots (contour threshold 0.002 au) for the lowest transition of **5'** (top) and substituted with **6'-H** (middle) and **6'** (bottom).

Table S 2. Comparison between theoretical and experimental wavelengths (nm) for **5'**, **6'-H** and **6'**. The theoretical values have been obtained with TD-DFT correcting the transition energies with SOS-CIS(D) or CC2. Both the absorption and emission wavelengths have been obtained in the vertical approximation. All values in acetonitrile.

Compound	Absorption			Emission			0-0 (=AFCP)		
	S/CIS(D)	CC2	Exp	S/CIS(D)	CC2	Exp	S/CIS(D)	CC2	Exp
5'	616	569	616	747	665	667	726	660	642
6'-H	566	537	590	675	618	654	666	617	619
6'	613	734	626	847	919	709	796	889	669

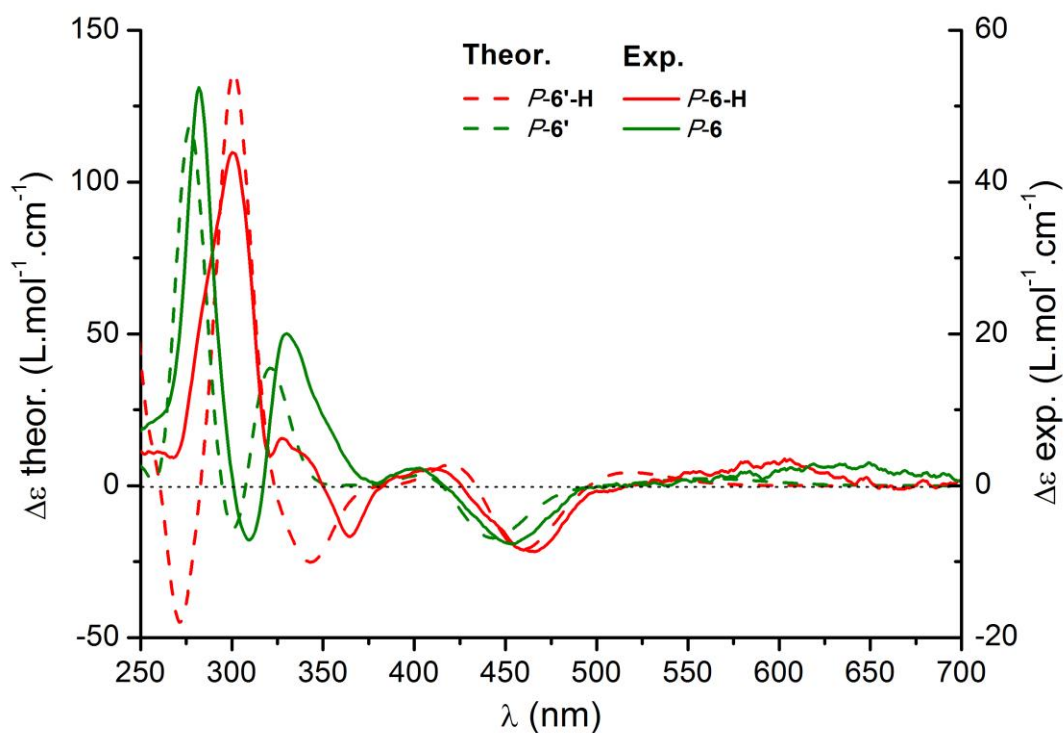


Figure S8. Experimental (plain) and simulated (dashed) ECD spectra simulated for the *P* enantiomer of **6/6-H** and **6'/6'-H**.

7. References

- (a) B. W. Laursen and F. C. Krebs, *Angew. Chem. Int. Ed.*, 2000, **39**, 3432-3434; (b) B. W. Laursen and F. C. Krebs, *Chem. Eur. J.*, 2001, **7**, 1773-1783; (c) C. Herse, D. Bas, F. C. Krebs, T. Bürgi, J. Weber, T. Wesolowski, B. W. Laursen and J. Lacour, *Angew. Chem. Int. Ed.*, 2003, **42**, 3162-3166; (d) T. J. Sørensen, M. F. Nielsen and B. W. Laursen, *ChemPlusChem*, 2014, **79**, 1030-1035; (e) I. Hernández Delgado, S. Pascal, A. Wallabregue, R. Duwald, C. Besnard, L. Guénée, C. Nançoz, E. Vauthey, R. C. Tovar, J. L. Lunkley, G. Muller and J. Lacour, *Chem. Sci.*, 2016, DOI: 10.1039/C6SC00614K.
- B. Laleu, P. Mobian, C. Herse, B. W. Laursen, G. Hopfgartner, G. Bernardinelli and J. Lacour, *Angew. Chem.*, 2005, **117**, 1913-1917.
- CrysalisPro Software system, Agilent Technologies UK Ltd., Oxford, UK.
- G. Sheldrick, *Acta Crystallogr. A*, 2008, **64**, 112-122.
- M. C. Burla, R. Caliandro, M. Camalli, B. Carrozzini, G. L. Casciaro, L. De Caro, C. Giacovazzo, G. Polidori and R. Spagna, *J. Appl. Crystallogr.*, 2005, **38**, 381-388.
- L. Palatinus and G. Chapuis, *J. Appl. Crystallogr.*, 2007, **40**, 786-790.
- O. V. Dolomanov, L. J. Bourhis, R. J. Gildea, J. A. K. Howard and H. Puschmann, *J. Appl. Crystallogr.*, 2009, **42**, 339-341.
- Frisch, M. J.; Trucks, G. W.; Schlegel, H. B.; Scuseria, G. E.; Robb, M. A.; Cheeseman, J. R.; Scalmani, G.; Barone, V.; Mennucci, B.; Petersson, G. A.; Nakatsuji, H.; Caricato, M.; Li, X.; Hratchian, H. P.; Izmaylov, A. F.; Bloino, J.; Zheng, G.; Sonnenberg, J. L.; Hada, M.; Ehara, M.; Toyota, K.; Fukuda, R.; Hasegawa, J.; Ishida, M.; Nakajima, T.; Honda, Y.; Kitao, O.; Nakai, H.; Vreven, T.; Montgomery, J. A., Jr.; Peralta, J. E.; Ogliaro, F.; Bearpark, M.; Heyd, J. J.; Brothers, E.; Kudin, K. N.; Staroverov, V. N.; Kobayashi, R.; Normand, J.; Raghavachari, K.; Rendell, A.; Burant, J. C.; Iyengar, S. S.; Tomasi, J.; Cossi, M.; Rega, N.; Millam, J. M.; Klene, M.; Knox, J. E.; Cross, J. B.; Bakken, V.; Adamo, C.; Jaramillo, J.; Gomperts, R.; Stratmann, R. E.; Yazyev, O.; Austin, A. J.; Cammi, R.; Pomelli, C.; Ochterski, J. W.; Martin, R. L.; Morokuma, K.; Zakrzewski, V. G.; Voth, G. A.; Salvador, P.; Dannenberg, J. J.; Dapprich, S.; Daniels, A. D.; Farkas, Ö.; Foresman, J. B.; Ortiz, J. V.; Cioslowski, J.; Fox, D. J. Gaussian 09, revision D.01; Gaussian, Inc.: Wallingford, CT, 2009.
- Y. Zhao and D. Truhlar, *Theor. Chem. Acc.*, 2008, **120**, 215-241.
- (a) D. Jacquemin, A. Planchat, C. Adamo and B. Mennucci, *J. Chem. Theory Comput.*, 2012, **8**, 2359-2372; (b) R. Li, J. Zheng and D. G. Truhlar, *Phys. Chem. Chem. Phys.*, 2010, **12**, 12697-12701; (c) M. Isegawa, R. Peverati and D. G. Truhlar, *J. Chem. Phys.*, 2012, **137**, 244104; (d) S. S. Leang, F. Zahariev and M. S. Gordon, *J. Chem. Phys.*, 2012, **136**, 104101; (e) A. Charaf-Eddin, A. Planchat, B. Mennucci, C. Adamo and D. Jacquemin, *J. Chem. Theory Comput.*, 2013, **9**, 2749-2760.
- A. D. Laurent and D. Jacquemin, *Int. J. Quant. Chem.*, 2013, **113**, 2019-2039.
- J. Tomasi, B. Mennucci and R. Cammi, *Chem. Rev.*, 2005, **105**, 2999-3094.
- (a) R. Cammi and B. Mennucci, *J. Chem. Phys.*, 1999, **110**, 9877-9886; (b) M. Cossi and V. Barone, *J. Chem. Phys.*, 2001, **115**, 4708-4717.
- M. Caricato, B. Mennucci, J. Tomasi, F. Ingrosso, R. Cammi, S. Corni and G. Scalmani, *J. Chem. Phys.*, 2006, **124**, 124520.
- B. Le Guennic and D. Jacquemin, *Acc. Chem. Res.*, 2015, **48**, 530-537.
- (a) D. Jacquemin, T. L. Bahers, C. Adamo and I. Ciofini, *Phys. Chem. Chem. Phys.*, 2012, **14**, 5383-5388; (b) T. Le Bahers, C. Adamo and I. Ciofini, *J. Chem. Theory Comput.*, 2011, **7**, 2498-2506.
- Y. Shao, L. F. Molnar, Y. Jung, J. Kussmann, C. Ochsenfeld, S. T. Brown, A. T. B. Gilbert, L. V. Slipchenko, S. V. Levchenko, D. P. O'Neill, R. A. DiStasio Jr, R. C. Lochan, T. Wang, G. J. O. Beran, N. A. Besley, J. M. Herbert, C. Yeh Lin, T. Van Voorhis, S. Hung Chien, A. Sodt, R. P. Steele, V. A. Rassolov, P. E. Maslen, P. P. Korambath, R. D. Adamson, B. Austin, J. Baker, E. F. C. Byrd, H.

- Dachsel, R. J. Doerksen, A. Dreuw, B. D. Dunietz, A. D. Dutoi, T. R. Furlani, S. R. Gwaltney, A. Heyden, S. Hirata, C.-P. Hsu, G. Kedziora, R. Z. Khalliulin, P. Klunzinger, A. M. Lee, M. S. Lee, W. Liang, I. Lotan, N. Nair, B. Peters, E. I. Proynov, P. A. Pieniazek, Y. Min Rhee, J. Ritchie, E. Rosta, C. David Sherrill, A. C. Simmonett, J. E. Subotnik, H. Lee Woodcock Iii, W. Zhang, A. T. Bell, A. K. Chakraborty, D. M. Chipman, F. J. Keil, A. Warshel, W. J. Hehre, H. F. Schaefer Iii, J. Kong, A. I. Krylov, P. M. W. Gill and M. Head-Gordon, *Phys. Chem. Chem. Phys.*, 2006, **8**, 3172-3191.
- 18 Turbomole V6.6 2014, a Development of University of Karlsruhe and Forschungszentrum Karlsruhe GmbH, 1989–2007, Turbomole GmbH. <http://www.turbomole.com>.